

ADVANCED TECHNIQUE FOR KALMAN FILTER ADJUSTMENT AND ITS IMPLEMENTATION ONBOARD OF "TABLESAT" MICROSATELLITE SERIES

D. Ivanov,^{*} N. Ivlev,[†] S. Karpenko,[‡] and M. Ovchinnikov[§]

In the paper we introduce the analytical approach that allows us to study the filter performance and it can be applied for quasi-stationary motion determination. The approach based on a computation of filter covariance matrix after convergence, and it allows us to estimate the influence of unaccounted perturbations on motion determination accuracy. Accuracy dependence on filter parameters and perturbation is analytically derived. The proposed advanced method for Kalman filter performance adjustment and study is applied for a set of the algorithms of "TabletSat" microsattellites series.

INTRODUCTION

Microsatellite attitude control requires determination of the attitude motion state vector. The state vector is determined by processing attitude sensors' measurements by on-board computer which has computational constrains because of the power limit of microsattellites. That is why recursive algorithms based on the Kalman filter are often applied. The Kalman filter uses linearized satellite attitude motion equations and sensor measurements to estimate state vector by mean square criteria. Due to computational limitaions, the motion equations cannot take into account all perturbations affecting the satellite and caused by environment and by actuators errors. It leads to attitude determination accuracy decreasing. So, there appears a problem of, so called, *unaccounted perturbations influence*.

Selection of motion model error and measurement noise statistics, commonly referred to as filter tuning, is a major implementation issue for the Kalman filter. This process can make a significant impact on the filter performance. Gelb¹ described the sensitivity of the steady-state covariance of a scalar Kalman filter to Kalman gain selection which illustrates the effect of filter tuning.

In practice, Kalman filter tuning is often an *ad hoc* process involving a considerable amount of trial-and-error to obtain a filter with desirable performance characteristics. Maybeck^{2, 3} and others suggested to tune a Kalman filter with a numerical minimization technique. Oshman et.al. used a Monte Carlo simulation technique to statistically assess the performance of the algorithm applied and to demonstrate its viability⁴. Oshman also used the genetic algorithms for the filter tuning⁵. Algorithms result in objective function minimization by varying set of filter parameters

^{*} PhD, Keldysh Institute of Applied Mathematics RAS, Juniour Researcher, Miusskaya Sq.4, Moscow, Russia.

[†] PhD Student, "SputniX" Ltd, Principal Engineer, Moscow, Berezhkovskaya naberazhnaya, 20-6, Moscow, Russia.

[‡] Mr., "SputniX" Ltd, Chief Technical Officer, Moscow, Berezhkovskaya naberazhnaya, 20-6, Moscow, Russia.

[§] Professor, Keldysh Institute of Applied Mathematics RAS, Head of Division Miusskaya Sq., 4, Moscow, Russia.

in simulations. However, the simulation takes a plenty of time, its results are stochastic and obtained minimum is local only. The numerical minimization technique applied in ⁶ is the downhill simplex method which is a function optimization algorithm available in several programming languages. It uses only function evaluations to fix a local minimum of the objective function. Here the objective function is the root mean square of the state estimation errors (estimate minus truth) which assumes “true” states are available.

Another approach to Kalman filter accuracy determination can be applied to steady-state motion analysis. It does not require the filter work simulations. In ^{7, 8} it is shown that filter covariance matrix asymptotical value can be obtained from the solution of a matrix quadratic equation. For the single-axis attitude estimator this equation is solved analytically in the explicit formulas ^{9,10}. In more common case the equation can be solved only numerically. Nevertheless, the considered approach cannot provide an estimation of unaccounted perturbation influence on the filter accuracy.

In the paper we introduce the analytical approach that allows us to study the filter performance and it can be applied for quasi-stationary motion analysis. The approach based on a computation of filter covariance matrix after convergence, and it allows to estimate the influence of unaccounted perturbations on motion determination accuracy. The main advantage of this approach is that it does not require the simulation of Kalman filter, consequently does not require too much computational time, the estimation of filter accuracy is an asymptotic value after convergence. Accuracy dependences on filter parameters and perturbation are analytically derived, and more reliable than ones derived by approaches described above.

Kalman filters have been widely used for spacecraft attitude determination. Star sensors ^{11, 12}, sun sensors ¹³, gyros ^{14, 15} and magnetometers ^{16,17} have been used for filter inputs. Attitude estimation algorithms using vector observation are presented in ^{18, 19}. For magnetometer and sun sensor use there a problem arises when magnetic field and Sun directions become collinear. In that case the three-axis attitude is non-observable. Actually, Kalman filter accuracy decreases when the angle between two vectors is getting small. In the paper this dependence is obtained analytically. The proposed advanced method for Kalman filter performance adjustment and study is applied for a set of the algorithms of "TabletSat" microsattellites series. "TabletSat" is a microsattelite platform for implementation of technological experiments in space which is developed and built by SputniX Ltd company.

"TABLESAT" MICROSATELLITE SERIES

The approach in designing small spacecraft applied by SputniX Ltd is based on the modular principle for satellite building with the use of generic service systems and payloads, which enables shaping scalable architecture and satellite functionality similar to LEGO set. The approach is based on open SxPA-specifications (SPUTNIX Plug-n-Play Architecture), describing mechanical, electrical and data interfaces between service systems and payloads.

Following this approach the TabletSat platform was designed. The basic unit of the TabletSat platform structure is a module weighting about 10 kg which was named 1U (U-UNIT). Other standard sizes (2U, 3U, 4U) having greater mass and electric power margin for payloads could be achieved by increasing the number of generic 1U modules. Selection of a form-factor (hexagonal prism) depends exclusively on capabilities and convenience of launching the platform as a secondary payload.

The technology and service systems being developed by SPUTNIX allow building microsattellites of 10 – 50kg of mass including payloads. It is also possible to build a microsattelite with the

mass up to 100kg. The microsatellite consists of unified elements, it is easy to assemble, integrate on the launch vehicle and be launched. After launching it is radio frequency compatible with a wide variety of ground control, telemetry and scientific information stations.

Depending on the mission requirements a specific set of ADCS actuators and sensors are installed on board TabletSat. To ensure the required motion it is necessary to develop a bank of attitude control and attitude determination algorithms. However, each algorithm has its own characteristics, parameters and constraints that need to identify and analyze the analytical theory and numerical study. As the first step of the algorithms verification it is necessary to mathematical modeling of their work with actuators and sensor parameters of microsatellite TabletSat. First satellite of the TabletSat series is a TabletSat-Aurora.

TabletSat-Aurora

Micro-satellite technology demonstrator TabletSat-Aurora (Figure 1) is designed by SPUTNIX and intended for tuning up the set of the following service systems:

- Three-axis orientation and stabilization system (flywheels, motors-gyros, star sensor and sun sensors, magnetometer, and angular rate sensor). Parameters of attitude determination sensor are listed in Table 1;
- Onboard GPS navigator;
- Onboard UHF telecommand and telemetry module;
- Onboard Pug-n-Play architecture based on SpaceWire bus;
- Onboard X-Band transmission system;
- LiFePO4 battery-powered supply system;
- Experimental PCB-based AsGa solar panel.

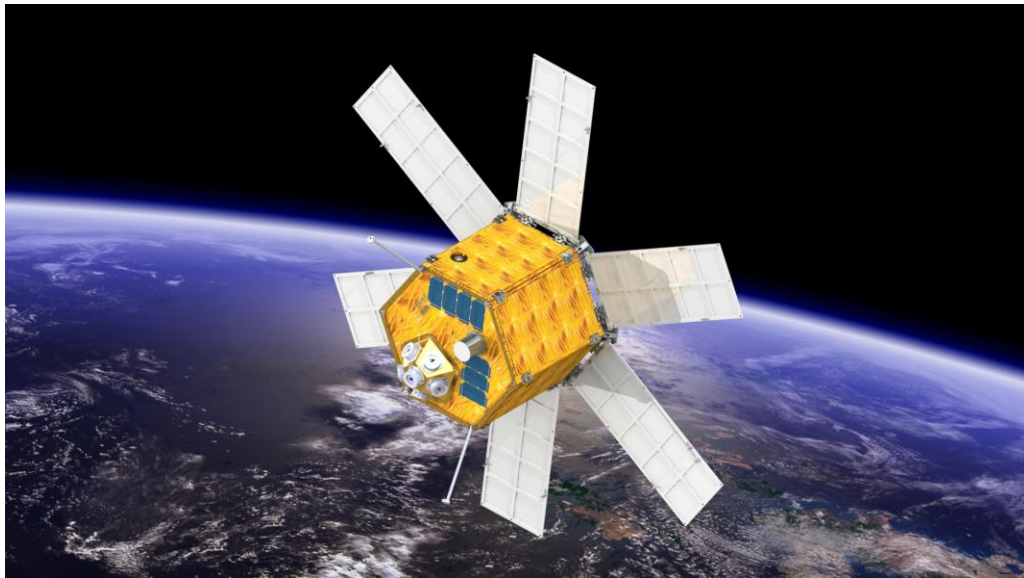


Figure 1. TabletSat-Aurora

Table 1. Attitude determination sensors parameters

Parameter	Magnetometer	Sun sensor	Angular velocity sensor	Star sensor
Instrument range	$\pm 200\,000$ nT	± 60 deg	± 250 deg/s	–
Mean-square error (σ)	250 nT	0.1 deg	0.005 deg/s	0.001 deg

The 2U-format microsatellite with the mass of about 25 kg will be launched in mid of 2014.

The spacecraft will be fitted with panchromatic photo- and video- camera operating in 430 – 950 μm spectral band as the primary payload to perform imagery of Earth surface.

KALMAN FILTER ADJUSTMENT TECHNIQUE

Kalman filter

First consider briefly a well-known standard extended Kalman filter algorithm formulation^{8,20}. Assume the satellite motion model is nonlinear,

$$\dot{\mathbf{x}} = \mathbf{f}(\mathbf{x}, t) + \mathbf{q} \quad (1)$$

where \mathbf{x} is a state vector, \mathbf{f} is a nonlinear function, \mathbf{q} is a dynamical noise of normal distribution with covariance matrix of motion model errors Q . Prediction of the state vector estimation $\hat{\mathbf{x}}_{k+1}^-$ (*a priori*) at the time t_{k+1} is calculated by integration of nonlinear equation (1) (without \mathbf{q} vector) using state vector $\hat{\mathbf{x}}_k^+$ at previous time step t_k . Discrete Riccati equation is used to obtain prediction of the error covariance matrix vector estimation P_{k+1}^- at the time t_{k+1} ,

$$P_{k+1}^- = \Phi_k P_k^+ \Phi_k^T + Q \quad (2)$$

where Φ_k is a transition matrix between states \mathbf{x}_k and \mathbf{x}_{k+1} , which is calculated by linearization equation (1) in the vicinity of $\hat{\mathbf{x}}_k^-$, P_k^+ is a error covariance matrix at t_k .

The *a posteriori* estimation is *a priori* estimation corrected by the measurements sampled. In general case the measurement vector \mathbf{z} nonlinearly depends on the state vector \mathbf{x} ,

$$\mathbf{z}_{k+1} = \mathbf{h}(\mathbf{x}_{k+1}^-, t_{k+1}) + \mathbf{r}. \quad (3)$$

Here \mathbf{h} is a nonlinear function, \mathbf{r} is the measurement noise vector with the covariance matrix R . The gain matrix K_k can be written as

$$K_{k+1} = P_{k+1}^- H_{k+1}^T [H_{k+1} P_{k+1}^- H_{k+1}^T + R]^{-1}. \quad (4)$$

where H_{k+1} is the sensitivity matrix calculated by linearization of measurement model (3) in the vicinity of $\hat{\mathbf{x}}_k^-$. The corrected (*a posteriori*) estimation \mathbf{x}_{k+1}^+ of the Kalman filter has the form

$$\mathbf{x}_{k+1}^+ = \mathbf{x}_{k+1}^- + K_{k+1} [\mathbf{z}_{k+1} - \mathbf{h}(\mathbf{x}_{k+1}^-, t_k)].$$

The *a posteriori* estimation for the error matrix has the form

$$P_{k+1}^+ = [E - K_{k+1} H_{k+1}] P_{k+1}^-$$

where E is an identity matrix.

Accuracy estimation at quasi stationary motion

The Kalman filter covariance matrix of errors P is a qualitative criterion of the state vector estimation. If the quantity of matrix P_k at the time t_k is known, one can calculate the state vector $\hat{\mathbf{x}}_k$ determination accuracy. However, the value of P_k depends on a number of factors like initial state vector \mathbf{x}_0 , initial value P_0 , covariance matrix of motion model error Q , measurement errors R , system dynamics. In addition, motion equation used by the Kalman filter does not include some disturbance torques with a complex mathematical model because it is rather difficult to implement it to on-board computer. Usually the influence of unaccounted perturbation on accuracy estimation is investigated by simulation of filter work. Such a Kalman filter study approach takes a lot of time for computing and its results are correct with a certain probability only.

Sometimes another Kalman filter study approach can be applied. If the satellite attitude motion is sufficiently slow (or the measurement sampling frequency is high enough) let us consider it as a quasi stationary and allow to be $\Phi_k = \Phi \approx const$, $H_k = H \approx const$. Then, determine the quasi-stationary motion as such a motion when the acting forces and the measurement model are close to be a constant during the time between sequential measurements. For the discrete extended Kalman filter one can calculate the covariance error matrix P_∞ value after convergence. So, the filter performance quality after transient process is investigated⁸. For this matrix values on two sequential steps should be equal,

$$P_\infty = P_k = P_{k-1},$$

Therefore, the following matrix equation

$$P_\infty = \left[E - (\Phi P_\infty \Phi^T + Q) H^T \left[H (\Phi P_\infty \Phi^T + Q) H^T + R \right]^{-1} H \right] (\Phi P_\infty \Phi^T + Q) \quad (5)$$

is valid. Note that all matrices in this equation are to be constant. Taking into account that matrix P_∞ is a symmetrical one, the considered nonlinear matrix equation can be rewritten as nonlinear equations with n unknown variables (i.e. elements of matrix P_∞). These equations can be solved, for example, by the Newton method.

Investigation of estimation accuracy dependence on unaccounted perturbations

Consider how to estimate influence of disturbances on the filter accuracy. The Kalman filter is developed for the linear motion and linear measurement models (or for linearized models) as follows

$$\mathbf{x}_{k+1} = \Phi_k \mathbf{x}_k + \mathbf{w}_k, \quad (6)$$

$$\mathbf{z}_k = H_k \mathbf{x}_k + \mathbf{v}_k. \quad (7)$$

However, the real system can be affected by unaccounted in the models perturbations. Let the vector $\boldsymbol{\chi}$ be a real vector of motion equation errors which is described also by its own equations

$$\begin{aligned} \mathbf{x}_{k+1} &= \Phi_k \mathbf{x}_k + \boldsymbol{\chi}_k, \\ \boldsymbol{\chi}_{k+1} &= \Gamma_k \boldsymbol{\chi}_k + \boldsymbol{\theta}_k, \end{aligned} \quad (8)$$

where Γ_k is a transition matrix of unaccounted perturbation vector $\boldsymbol{\chi}$, $\boldsymbol{\theta}_k$ is a noise of normal distribution with covariance errors matrix Θ_k .

The real measurement model can be also different from the one used in Kalman filter:

$$\begin{aligned} \mathbf{z}_k &= H_k \mathbf{x}_k + \mathbf{v}_k, \\ \mathbf{v}_{k+1} &= Y_k \mathbf{v}_k + \boldsymbol{\rho}_k. \end{aligned} \quad (9)$$

Here \mathbf{v}_k the real measurement noise vector, Y_k is transition matrix of error vector, $\boldsymbol{\rho}_k$ is the normally distributed error of \mathbf{v}_k with covariance error matrix Ξ_k .

So, there is a task to estimate influence of unaccounted disturbances in (8), (9) on the accuracy of Kalman filter which uses models (6) and (7)²¹. Consider a new state vector $\boldsymbol{\xi} = (\mathbf{x}^T, \boldsymbol{\chi}^T, \mathbf{v}^T)^T$. Construct the Kalman filter for the state vector $\boldsymbol{\xi}$. The propagated value of the error matrix $P_{\boldsymbol{\xi},j+1}^-$ is calculated by the equation

$$P_{\boldsymbol{\xi},k}^- = \Phi_{\boldsymbol{\xi},k} P_{\boldsymbol{\xi},k-1}^+ \Phi_{\boldsymbol{\xi},k}^T + Q_{\boldsymbol{\xi},k}, \quad (10)$$

similar to (2), where

$$\Phi_{\boldsymbol{\xi},k} = \begin{pmatrix} \Phi_k & E & 0 \\ 0 & \Gamma_k & 0 \\ 0 & 0 & Y_k \end{pmatrix}, \quad Q_{\boldsymbol{\xi},k} = \begin{pmatrix} 0 & 0 & 0 \\ 0 & \Theta_k & 0 \\ 0 & 0 & \Xi_k \end{pmatrix}.$$

At *a posteriori* estimation only a state vector \mathbf{x} is corrected while vectors $\boldsymbol{\chi}$ and \mathbf{v} remain

$$\hat{\mathbf{x}}_k^+ = (E - K_k H_k) \hat{\mathbf{x}}_k^- - K_k \boldsymbol{\chi}_k,$$

$$\boldsymbol{\chi}_k^+ = \boldsymbol{\chi}_k^-,$$

$$\mathbf{v}_k^+ = \mathbf{v}_k^-.$$

The *a posteriori* estimation for the error matrix has the form

$$P_{\boldsymbol{\xi},k}^+ = C_k P_{\boldsymbol{\xi},k}^- C_k^T \quad (11)$$

where

$$C_k = \begin{pmatrix} E - K_k H_k & 0 & -K_k \\ 0 & E & 0 \\ 0 & 0 & E \end{pmatrix},$$

K_k is a gain matrix of the Kalman filter from (4).

So, if the covariance error matrix $P_{\xi,k}^+$ is available, one can calculate the estimation accuracy of state vector \mathbf{x} using the corresponding part of the matrix. This accuracy takes into account real dynamical equation (8) and real measurement model (9).

If the motion is close to quasi stationary then one can calculate the asymptotical value of error matrix $P_{\xi,\infty}$

$$P_{\xi,\infty} = C_{\xi} \left[\Phi_{\xi} P_{\xi,\infty} \Phi_{\xi}^T + Q_{\xi} \right] C_{\xi}^T. \quad (12)$$

If the real motion equation and real measurement model differ from the ones used by Kalman filter, the motion error matrix Q and the measurement error matrix R become parameters of the filter. Aim of the filter adjustment is to choose Q and R to minimize accuracy of the state vector \mathbf{x} estimation

$$\{Q, R\} = \arg \min(\text{tr } P_{\xi,\infty}). \quad (13)$$

Minimization problem (13) can be solved following the way. One can assume that the errors are independent and the error matrices Q , R are diagonal. Depending on the problem only matrix Q can be chosen as a parameter. So, minimization problem (13) can be solved by gradient descent method calculating the accuracy in certain parameters area with defined step.

Thus, proposed Kalman filter adjustment technique for quasi stationary motion consists of three stages:

- Calculation the asymptotical value of error matrix P_{∞} (5) and gain matrix K_{∞} (4).
- Obtaining the error matrix $P_{\xi,\infty}$ from equation (12).
- Solving the minimization problem (13).

TABLESAT KALMAN FILTERS INVESTIGATION

Let us apply proposed Kalman filter adjustment technique for a set of filters. Consider twelve different algorithms which use measurements of the star, angular velocity, sun sensors and magnetometer. The bank of algorithms is developed for state vector estimation in all the situations, some of the sensors failures and also for calibration.

Dynamical motion equation

Assume the satellite dynamical motion equation take into account only control torque from reaction wheels and gravitational torque

$$J\dot{\boldsymbol{\omega}} = -\dot{\mathbf{h}} + \frac{3\mu}{R^3}(\boldsymbol{\eta} \times J\boldsymbol{\eta}) - \boldsymbol{\omega} \times (J\boldsymbol{\omega} + \mathbf{h}) \quad (14)$$

where $\boldsymbol{\omega} = [\omega_x \ \omega_y \ \omega_z]^T$ is a vector of angular velocity of body-fixed frame relatively Earth centered inertial (ECI) frame, J is a tensor of inertia, $\boldsymbol{\eta} = [\eta_x \ \eta_y \ \eta_z]^T$ is the local unit vector normal to the plane of orbit in the body-fixed frame, $\mu = GM_s$ is Earth's gravitational constant and r is the distance from the Earth center to the satellite center of mass, R is the distance to the Earth center, \mathbf{h} is a reaction wheel momentum, $\dot{\mathbf{h}}$ control reaction wheels torque, which is equal to

$$\dot{\mathbf{h}} = K_\alpha \boldsymbol{\lambda}_{rel} + K_\omega (\tilde{\boldsymbol{\omega}} - \tilde{\boldsymbol{\omega}}_0) - \boldsymbol{\omega} \times (J\boldsymbol{\omega} + \mathbf{h}),$$

$\boldsymbol{\lambda}_{rel}$ is a vector part of the quaternion $\Lambda_{rel} = [\boldsymbol{\lambda}_{rel}^T \ \lambda_{rel}^0]^T = \Lambda_0^{-1}\Lambda$, where $\Lambda = [\boldsymbol{\lambda}^T \ \lambda^0]^T$ representing the transition from the local-vertical-local-horizontal (LVLH) frame to the body-fixed frame, Λ_0 is a desired orientation, $\tilde{\boldsymbol{\omega}}$ is a vector of angular velocity of body-fixed frame relatively LVLH, $\tilde{\boldsymbol{\omega}}_0$ is the desired angular velocity, $K_\alpha = \text{diag}(k_\alpha^1, k_\alpha^2, k_\alpha^3)$, $K_\omega = \text{diag}(k_\omega^1, k_\omega^2, k_\omega^3)$ are diagonal matrices of control parameters of reaction wheels. Let us write the kinematic relations as

$$\dot{\Lambda} = \frac{1}{2}\Omega\Lambda \quad (15)$$

where

$$\Omega = \begin{pmatrix} \tilde{W} & \tilde{\boldsymbol{\omega}} \\ -\tilde{\boldsymbol{\omega}}^T & 0 \end{pmatrix},$$

\tilde{W} is a skew-symmetric matrix of $\tilde{\boldsymbol{\omega}}$.

The vector part of the quaternion and the angular velocity of the body-fixed frame with respect to the ECI frame $\mathbf{x} = [\boldsymbol{\lambda}^T \ \boldsymbol{\omega}^T]^T$ are taken as the vector of estimated values. Let us linearize the equations of motion in the vicinity of the current motion $\mathbf{x}(t)$. Rewrite equations (14) and (15) as

$$\frac{d}{dt}\delta\mathbf{x}(t) = F(t)\delta\mathbf{x}(t)$$

where $\delta\mathbf{x}(t)$ is a small increment of the state vector, and $F(t)$ is a linearized matrix of the motion equations in the vicinity of $\hat{\mathbf{x}}(t)$:

$$F = \begin{pmatrix} -W_\omega & \frac{1}{2}E \\ J^{-1}(kF_g - K_\alpha W_{\Lambda_{rel}}) & -J^{-1}K_\omega \end{pmatrix}.$$

Here W_ω is a skew-symmetric matrix of $\boldsymbol{\omega}$, $k = 6\mu/R^3$,

$$W_{\Lambda_{rel}} = \begin{pmatrix} \lambda_{rel}^0 & -\lambda_{rel}^3 & \lambda_{rel}^2 \\ \lambda_{rel}^3 & \lambda_{rel}^0 & -\lambda_{rel}^1 \\ -\lambda_{rel}^2 & \lambda_{rel}^1 & \lambda_{rel}^0 \end{pmatrix},$$

$F_g = W_{\eta} J W_{\eta} - W_{J\eta} W_{\eta}$ is a matrix of linearized gravitational torque, W_{η} and $W_{J\eta}$ are skew-symmetric matrices of $\boldsymbol{\eta}$ and $J\boldsymbol{\eta}$ correspondingly.

Different measurement models (3) correspond to different set of sensors which measurements are used by the filter. The sensitivity matrix H for each model differ as well, there expressions are shown in Appendix A. The measurement errors matrices R are ordinarily diagonal and correspond to the sensor error characteristics given in Table 1. For instance, for the Kalman filter based on magnetometer and sun sensors the measurement vector consists of the magnetic field \mathbf{b} and Sun direction \mathbf{s} vectors in the body-fixed frame,

$$\mathbf{z}_k = [\mathbf{b}_k \quad \mathbf{s}_k]^T,$$

The vector \mathbf{h} from measurement models (3) can be written as

$$\mathbf{h} = \left[\left(A(\hat{\Lambda}_k^-) \mathbf{b}_o \right)^T \quad \left(A(\hat{\Lambda}_k^-) \mathbf{s}_o \right)^T \right]^T,$$

where A is the direction cosine matrix for the transition from the body-fixed to the LVLH frame written in terms of the quaternion estimation, \mathbf{b}_o and \mathbf{s}_o are vectors of the geomagnetic field and the Sun direction written in the LVLH frame, respectively.

Linearize the measurement model,

$$\delta \mathbf{z}(t) = H(t) \delta \mathbf{x}(t)$$

where $\delta \mathbf{z}(t)$ is the small increment of measurements in case of small change of the state vector $\delta \mathbf{x}(t)$ at the time t , $H(t)$ is the linearized matrix of measurements as follows

$$H = \begin{pmatrix} W_{\mathbf{b}} & \mathbf{0}_{3 \times 3} \\ W_{\mathbf{s}} & \mathbf{0}_{3 \times 3} \end{pmatrix}$$

where $W_{\mathbf{b}}$, $W_{\mathbf{s}}$ are skew-symmetric matrices of propagation of measurements $\hat{\mathbf{b}} = A(\hat{\Lambda}_k^-) \mathbf{b}_o$, $\hat{\mathbf{s}} = A(\hat{\Lambda}_k^-) \mathbf{s}_o$ correspondingly.

Filters with calibration

Measurement errors of the sensors generally consist of the normally distributed part and of systematic error (bias). The biases can be obtained by the laboratory calibration tests before the satellite launch. Unfortunately some of the sensors biases depend on bad-determined conditions and can slowly change. The most critical problem is to estimate biases of magnetometer and angular velocity sensor measurements. Magnetometer measures both the geomagnetic field and also magnetic field of on-board devices and satellite boards current. Angular velocity sensor bias can depend on fluctuation of power supply voltage. The problem can be solved by taking into account

the sensors biases in the measurement model and by estimating its values by Kalman filter. In the case the sensor biases become a part of the state vector \mathbf{x} .

Usually it is assumed the sensors biases derivative has normal distribution. Let us use the following angular velocity sensor measurement model

$$\begin{aligned}\tilde{\boldsymbol{\omega}} &= \boldsymbol{\omega} + \Delta\boldsymbol{\omega} + \boldsymbol{\eta}_{\boldsymbol{\omega}}, \\ \Delta\dot{\boldsymbol{\omega}} &= \boldsymbol{\eta}_{\Delta\boldsymbol{\omega}},\end{aligned}$$

where $\tilde{\boldsymbol{\omega}}$ is a measurement vector of angular velocity, $\boldsymbol{\omega}$ is a true value of angular velocity, $\Delta\boldsymbol{\omega}$ is a angular velocity bias, $\boldsymbol{\eta}_{\boldsymbol{\omega}}$ and $\boldsymbol{\eta}_{\Delta\boldsymbol{\omega}}$ are normally distributed errors. Use similar magnetometer measurement model

$$\begin{aligned}\tilde{\mathbf{b}} &= A(\hat{\Lambda}_k^-)\mathbf{b}_o + \Delta\mathbf{b} + \boldsymbol{\eta}_{\mathbf{b}}, \\ \Delta\dot{\mathbf{b}} &= \boldsymbol{\eta}_{\Delta\mathbf{b}},\end{aligned}$$

where $\tilde{\mathbf{b}}$ is a measurement vector of magnetometer, \mathbf{b} is a true value of geomagnetic filed, $\Delta\mathbf{b}$ is a magnetometer measurement bias, $\boldsymbol{\eta}_{\mathbf{b}}$ and $\boldsymbol{\eta}_{\Delta\mathbf{b}}$ are normally distributed errors.

The sensitivity matrices H for the filters estimating $\Delta\boldsymbol{\omega}$ and $\Delta\mathbf{b}$ are shown in Appendix A.

Filters investigation by proposed technique

The equation of satellite motion (14) takes into account only the gravitational and control torques. Though the satellite can be pretreated by other torques as undesirable magnetic torque by on-board devices, torque by sun light pressure, solar panel vibration, aerodynamic torque, reaction wheels control errors etc. All of these perturbation torques are not included in dynamical model (14) because of its model complexity and its infinitesimality. Nevertheless, it is necessary to estimate its influence on the filter accuracy and performance.

Assume the sum of the perturbation torques is of a normal distribution with a covariance matrix Q . Let the motion equation model errors be not correlated and then the matrix Q is diagonal. Also, we suppose the errors corresponding to kinematical equation are the same for all components of quaternion vector part, and so for dynamical equation. So, let us consider the following matrix Q

$$Q = \text{diag}(q_{\lambda}^2, q_{\lambda}^2, q_{\lambda}^2, q_{\omega}^2, q_{\omega}^2, q_{\omega}^2)$$

where q_{λ}^2 and q_{ω}^2 are the dispersions of the vector-part quaternion error and of the angular velocity vector error correspondingly.

To estimate the filter accuracy let us calculate asymptotical value of error matrix P_{∞} from equation (5) and consider the diagonal elements p_{ii} of the matrix. An estimation of the mean square error of quaternion determination is $\sigma_{\lambda} = \sqrt{\max(p_{11}, p_{22}, p_{33})}$ and an estimation of the mean square error of angular velocity determination is $\sigma_{\omega} = \sqrt{\max(p_{44}, p_{55}, p_{66})}$.

Consider as an example investigation of the Kalman filter based on magnetometer and sun sensor measurements. Figures 2a and 2b demonstrate the accuracy of attitude determination (in

angles) and of angular velocity which depend on dynamical noise parameters q_λ and q_ω . One can see from Figure 2 that the accuracies of attitude and angular velocity are increasing when the noise intensities q_λ and q_ω are decreasing. It is rather obvious results since if there is no dynamical noise in the motion equation then the asymptotical value of error will converge to zero.

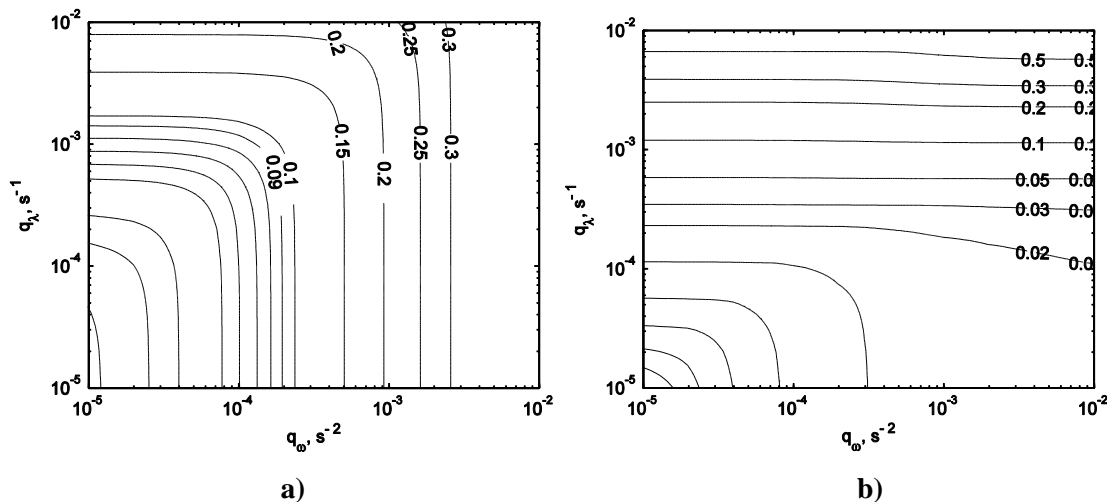


Figure 2. Attitude (a) and angular velocity (b) determination accuracy dependence on parameters q_λ and q_ω under $\mathbf{b}_o \perp \mathbf{s}_o$. Contours correspond to Euler angles accuracy levels in degree (a) and to angular velocity accuracy in degree per second (b).

Consider how the filter accuracy depends on perturbations unaccounted in motion equation. To estimate this dependence assume the unaccounted perturbation to be a constant and the real equation of motion (8) is following:

$$\begin{aligned} \mathbf{x}_{k+1} &= \Phi_k \mathbf{x}_k + \boldsymbol{\chi}_k, \\ \boldsymbol{\chi}_{k+1} &= E \boldsymbol{\chi}_k + \boldsymbol{\theta}_k, \end{aligned} \quad (16)$$

where E is an identity matrix, $\boldsymbol{\theta}$ is a normally distributed part of perturbation. Assume the perturbation vector $\boldsymbol{\chi}$ to be

$$\boldsymbol{\chi} = \left[d\Delta t^2 / 2 \quad d\Delta t^2 / 2 \quad d\Delta t^2 / 2 \quad d\Delta t \quad d\Delta t \quad d\Delta t \right]^T$$

where d is a constant, which defines the perturbation torque. Parameter d can be estimated as a maximum of possible unaccounted perturbation torque. In that case one can study the filter performance under the worst conditions. We estimated the maximum of perturbation torques as $8 \cdot 10^{-7}$ Nm for TabletSat microsattellites, that corresponds to parameter $d = 10^{-6} \text{ c}^{-2}$. Assume the normally distributed error $\boldsymbol{\theta}$ have covariance matrix

$$\mathbf{M}[\boldsymbol{\theta} \boldsymbol{\theta}^T] = \Theta = \text{diag}(10^{-14}, 10^{-14}, 10^{-14}, 10^{-14}, 10^{-14}, 10^{-14}).$$

In the case of real dynamical equation (16) the parameters q_λ and q_ω are not a dynamical noise parameters and it becomes just a Kalman filter adjustment parameters.

Consider the filter accuracy dependence on the parameters q_λ and q_ω when the magnetic field vector is perpendicular to Sun direction $\mathbf{b}_o \perp \mathbf{s}_o$ (Figure 3). The maximum of accuracy achieves at $q_\lambda = 8 \cdot 10^{-4} \text{ c}^{-1}$, $q_\omega = 2 \cdot 10^{-3} \text{ c}^{-2}$ and equals to $\sigma_\varphi = 0.12$ degree for attitude determination and $\sigma_\omega = 0.009$ for angular velocity determination. Figure 4 shows the errors of Euler angles and angular velocity estimation by Kalman filter work simulation with parameters q_λ and q_ω obtained above. One can see that the errors are very close to the ones calculated by theory. Figure 5 demonstrates how the best accuracy depends on perturbation value under $\mathbf{b}_o \perp \mathbf{s}_o$.

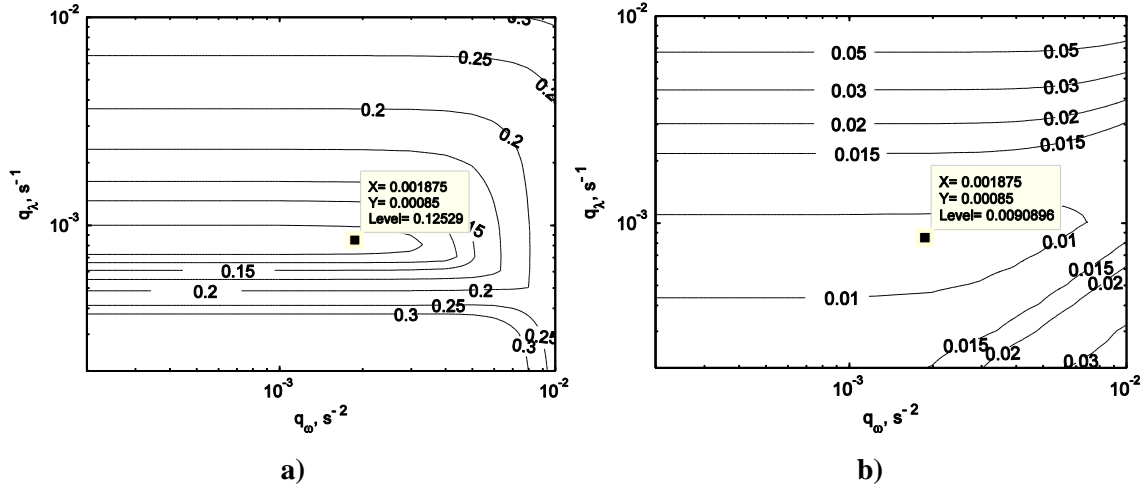


Figure 3. Attitude (a) and angular velocity (b) determination accuracy dependence on parameters q_λ and q_ω under $\mathbf{b}_o \perp \mathbf{s}_o$ and constant perturbation torque $8 \cdot 10^{-7} \text{ Nm}$. Contours correspond to Euler angles accuracy levels in degree (a) and to angular velocity accuracy in degree per second (b).

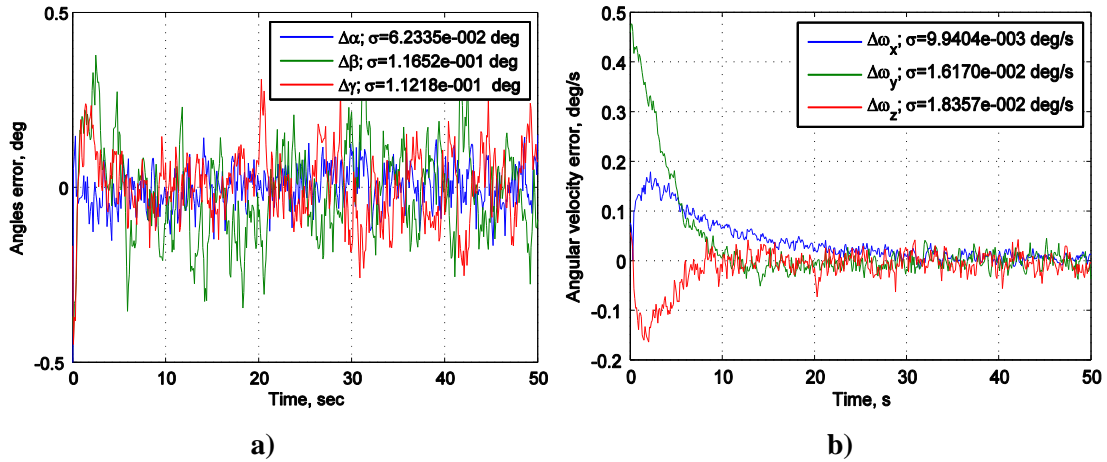


Figure 4. Attitude (a) and angular velocity (b) errors during Kalman filter work simulation with parameters $q_\lambda = 8 \cdot 10^{-4} \text{ c}^{-1}$, $q_\omega = 2 \cdot 10^{-3} \text{ c}^{-2}$ under $\mathbf{b}_o \perp \mathbf{s}_o$ and constant perturbation torque $8 \cdot 10^{-7} \text{ Nm}$.

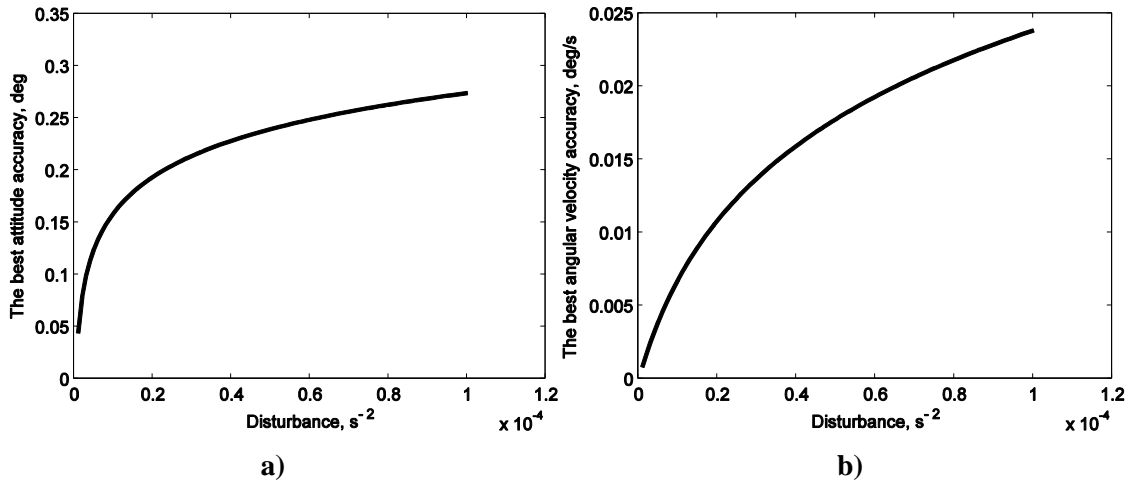


Figure 5. The best attitude (a) and angular velocity (b) determination accuracy dependence on perturbation torque under $\mathbf{b}_o \perp \mathbf{s}_o$ and constant. Contours correspond to Euler angles accuracy levels in degree (a) and to angular velocity accuracy in degree per second (b).

However, the accuracy decreases when angle between \mathbf{b}_o and \mathbf{s}_o far enough from 90 degree value. It is caused by the fact that the three-axis attitude has no observability when two measured vectors become collinear. The closer two vectors to be collinear the worse the filter estimation accuracy. Figure 6 shows this dependence obtained by the proposed approach of the filter study. As a result of this study if during the satellite exploitation the angle between \mathbf{b}_o and \mathbf{s}_o is less than 10 degree or more then 170 degree the accuracy of Euler angles estimation is unsatisfactory, and the TabletSat should switch its attitude control mode, for example, to a one-axis orientation to the Sun (for battery charging) which uses sun sensor measurements only.

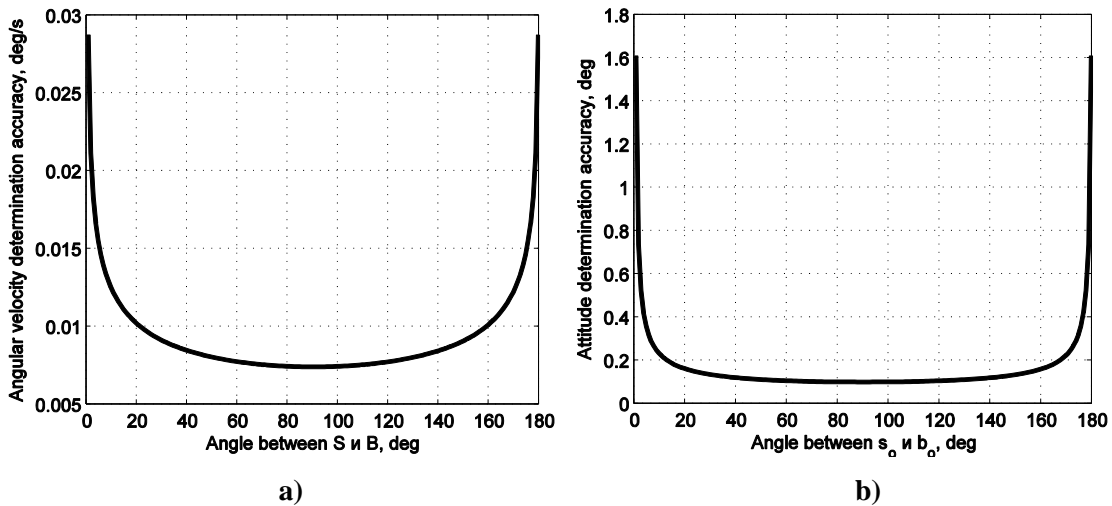


Figure 6. The best attitude (a) and angular velocity (b) determination accuracy dependence on angle between \mathbf{b}_o and \mathbf{s}_o under constant perturbation torque $8 \cdot 10^{-7}$ Nm. Contours correspond to Euler angles accuracy levels in degree (a) and to angular velocity accuracy in degree per second (b).

Consider how the unaccounted magnetometer bias affects an attitude determination accuracy. Let the real measurement model (9) to be as following:

$$\begin{aligned}\mathbf{z}_k &= \mathbf{h}(\mathbf{x}_k, t_k) + \mathbf{v}_k, \\ \mathbf{v}_{k+1} &= E\mathbf{v}_k + \boldsymbol{\rho}_k,\end{aligned}$$

where $\mathbf{v} = [\Delta b \ \Delta b \ \Delta b \ 0 \ 0 \ 0]^T$ is a vector of a biases, Δb is a vector of magnetometer bias, $\boldsymbol{\rho}_k$ is a normally distributed error with covariance matrix R . Attitude accuracy dependence on unaccounted magnetometer bias is presented in Figure 7.

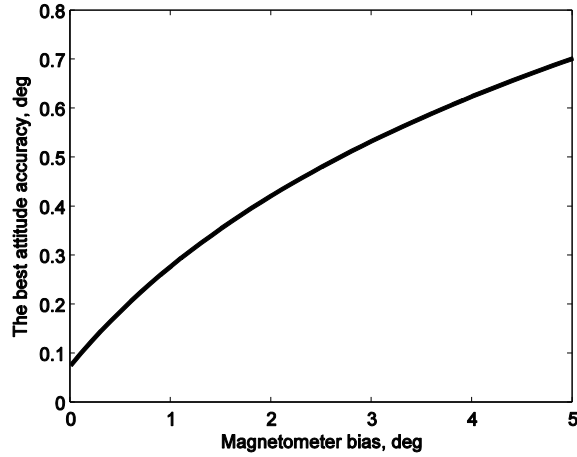


Figure 7. Attitude determination accuracy dependence on unaccounted magnetometer bias

One of the way to solve the problem of unaccounted magnetometer bias is to the extend state vector \mathbf{x} by Δb . The Figure 8 presents the bias estimation by the Kalman filter based on magnetometer, sun sensor and angular velocity sensor measurements. Initially the bias value error was about 0.1 rad and after 50 seconds the bias value converges to a real value.

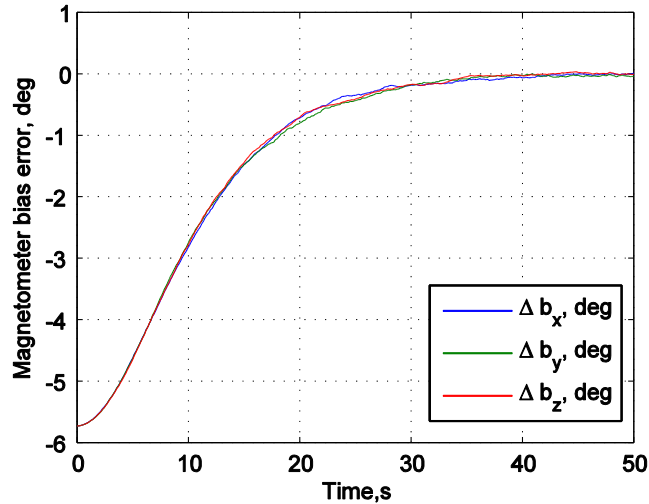


Figure 8. Estimation of magnetometer bias

So, the results of the Kalman filters based on different sets of sensors are presented in Table 2. The study was performed for the case when unaccounted torque is about $8 \cdot 10^{-7}$ Nm. The values of the attitude and the angular velocity determination accuracy are just an asymptotical estimation of the filter accuracy. Nevertheless its values can be used as a filter performance estimation.

Table 2. Results of the Kalman filter adjustment

Sensors	Measurement vector	State vector	Adjustment parameters $q_\lambda[s^{-1}]$ and $q_\omega[s^{-2}]$	Attitude and angular velocity determination accuracy
Star sensor, gyro, magnetometer, sun sensors	$\begin{pmatrix} \lambda \\ \omega \\ \mathbf{b} \\ \mathbf{s} \end{pmatrix}$	$\begin{pmatrix} \lambda \\ \omega \end{pmatrix}$	$1 \cdot 10^{-6}$, $1.2 \cdot 10^{-5}$	$5 \cdot 10^{-4}$ deg, $4 \cdot 10^{-4}$ deg/s
Star sensor, gyro, magnetometer	$\begin{pmatrix} \lambda \\ \omega \\ \mathbf{b} \end{pmatrix}$	$\begin{pmatrix} \lambda \\ \omega \end{pmatrix}$	$1 \cdot 10^{-6}$, $1.2 \cdot 10^{-5}$	$5 \cdot 10^{-4}$ deg, $4 \cdot 10^{-4}$ deg/s
Star sensor, magnetometer, sun sensors	$\begin{pmatrix} \lambda \\ \mathbf{b} \\ \mathbf{s} \end{pmatrix}$	$\begin{pmatrix} \lambda \\ \omega \end{pmatrix}$	$1 \cdot 10^{-6}$, $1.2 \cdot 10^{-5}$	$7 \cdot 10^{-4}$ deg, $6 \cdot 10^{-4}$ deg/s
Star sensor, magnetometer	$\begin{pmatrix} \lambda \\ \mathbf{b} \end{pmatrix}$	$\begin{pmatrix} \lambda \\ \omega \\ \Delta \mathbf{b} \end{pmatrix}$	$1 \cdot 10^{-6}$, $1.2 \cdot 10^{-5}$, $1 \cdot 10^{-4}$ ($q_{\Delta b}$)	$7 \cdot 10^{-4}$ deg, $6 \cdot 10^{-4}$ deg/s, 80 T ($\sigma_{\Delta b}$)
Magnetometer, sun sensors, gyro	$\begin{pmatrix} \mathbf{b} \\ \mathbf{s} \\ \omega \end{pmatrix}$	$\begin{pmatrix} \lambda \\ \omega \end{pmatrix}$	$5 \cdot 10^{-5}$, $5 \cdot 10^{-4}$	$2 \cdot 10^{-2}$ deg, $4 \cdot 10^{-3}$ deg/s
		$\begin{pmatrix} \lambda \\ \omega \\ \Delta \omega \end{pmatrix}$	$1 \cdot 10^{-6}$, $3 \cdot 10^{-3}$, $1 \cdot 10^{-6}$ ($q_{\Delta \omega}$)	$2 \cdot 10^{-2}$ deg, $4 \cdot 10^{-3}$ deg/s, $5 \cdot 10^{-4}$ deg/s ($\sigma_{\Delta \omega}$)
		$\begin{pmatrix} \lambda \\ \omega \\ \Delta \mathbf{b} \end{pmatrix}$	$5 \cdot 10^{-8}$, $3 \cdot 10^{-3}$, $5 \cdot 10^{-1}$ ($q_{\Delta b}$)	$5 \cdot 10^{-2}$ deg, $4 \cdot 10^{-3}$ deg/s, 400 T ($\sigma_{\Delta b}$)
Star sensor, gyro	$\begin{pmatrix} \lambda \\ \omega \end{pmatrix}$	$\begin{pmatrix} \lambda \\ \omega \end{pmatrix}$	$1 \cdot 10^{-6}$, $1.2 \cdot 10^{-5}$	$5 \cdot 10^{-4}$ deg, $4 \cdot 10^{-4}$ deg/s

		$\begin{pmatrix} \lambda \\ \omega \\ \Delta\omega \end{pmatrix}$	$1 \cdot 10^{-6},$ $1.2 \cdot 10^{-5},$ $1 \cdot 10^{-4} (q_{\Delta\omega})$	$5 \cdot 10^{-4} \text{ deg},$ $4 \cdot 10^{-4} \text{ deg/s},$ $3 \cdot 10^{-3} \text{ deg/s}$ $(\sigma_{\Delta\omega})$
Magnetometer, sun sensors	$\begin{pmatrix} \mathbf{b} \\ \mathbf{s} \end{pmatrix}$	$\begin{pmatrix} \lambda \\ \omega \end{pmatrix}$	$5 \cdot 10^{-4},$ $2 \cdot 10^{-3}$	$1.2 \cdot 10^{-1} \text{ deg},$ $2 \cdot 10^{-2} \text{ deg/s},$
Magnetometer, gyro	$\begin{pmatrix} \mathbf{b} \\ \omega \end{pmatrix}$	$\begin{pmatrix} \lambda \\ \omega \end{pmatrix}$	$1 \cdot 10^{-6},$ $5 \cdot 10^{-3}$	$2 \cdot 10^{-1} \text{ deg},$ $5 \cdot 10^{-3} \text{ deg/s},$
Star sensor	λ	$\begin{pmatrix} \lambda \\ \omega \end{pmatrix}$	$1 \cdot 10^{-6},$ $1.2 \cdot 10^{-5}$	$8 \cdot 10^{-4} \text{ deg},$ $6 \cdot 10^{-4} \text{ deg/s}$

CONCLUSION

The proposed method of Kalman filter performance study is an effective instrument for accuracy analysis and filter tuning in quasi-stationary satellite motion case. The approach allows to estimate the influence of unaccounted perturbation on a motion determination accuracy. The main advantage of this approach is that it does not require the simulation of Kalman filter, consequently does not require a lot of computational time, the estimation of filter accuracy is an asymptotic value after convergence. Accuracy dependence on filter parameters and perturbations is derived analytically, and is more reliable than one derived by known investigation approaches. It should be emphasized that the method can be applied only to the quasi-stationary motion when the acting forces and the measurement model are close to be a constant during the time interval between sequential measurements. The proposed advanced method for Kalman filter performance adjustment and study is applied for a set of the algorithms of "TabletSat" microsattellites series.

ACKNOWLEDGMENTS

This study was conducted in the framework of the Contract 1226/11-1 with SputniX Ltd., supported by the Russian Foundation for Basic Research (Grants 12-01-33045, 13-01-00665 and 14-01-31313) and the Ministry of Education and Science of the Russian Federation.

APPENDIX: SENSITIVITY MATRICES FOR KALMAN FILTERS BASED ON DIFFERENT SETS OF SENSORS

Sensors	Measurement vector	State vector	Sensitivity matrix H
Star sensor, gyro, magnetometer, sun sensors	$\begin{pmatrix} \lambda \\ \omega \\ \mathbf{b} \\ \mathbf{s} \end{pmatrix}$	$\begin{pmatrix} \lambda \\ \omega \end{pmatrix}$	$\begin{pmatrix} E_{3 \times 3} & 0_{3 \times 3} \\ 0_{3 \times 3} & E_{3 \times 3} \\ W_{\mathbf{b}} & 0_{3 \times 3} \\ W_{\mathbf{s}} & 0_{3 \times 3} \end{pmatrix}$

Star sensor, gyro, magnetometer	$\begin{pmatrix} \lambda \\ \omega \\ \mathbf{b} \end{pmatrix}$	$\begin{pmatrix} \lambda \\ \omega \end{pmatrix}$	$\begin{pmatrix} E_{3 \times 3} & 0_{3 \times 3} \\ 0_{3 \times 3} & E_{3 \times 3} \\ W_{\mathbf{b}} & 0_{3 \times 3} \end{pmatrix}$
Star sensor, magnetometer, sun sensors	$\begin{pmatrix} \lambda \\ \mathbf{b} \\ \mathbf{s} \end{pmatrix}$	$\begin{pmatrix} \lambda \\ \omega \end{pmatrix}$	$\begin{pmatrix} E_{3 \times 3} & 0_{3 \times 3} \\ W_{\mathbf{b}} & 0_{3 \times 3} \\ W_{\mathbf{s}} & 0_{3 \times 3} \end{pmatrix}$
Star sensor, magnetometer	$\begin{pmatrix} \lambda \\ \mathbf{b} \end{pmatrix}$	$\begin{pmatrix} \lambda \\ \omega \\ \Delta \mathbf{b} \end{pmatrix}$	$\begin{pmatrix} E_{3 \times 3} & 0_{3 \times 3} & 0_{3 \times 3} \\ W_{\mathbf{b}} & 0_{3 \times 3} & E_{3 \times 3} \end{pmatrix}$
Magnetometer, sun sensors, gyro	$\begin{pmatrix} \mathbf{b} \\ \mathbf{s} \\ \omega \end{pmatrix}$	$\begin{pmatrix} \lambda \\ \omega \end{pmatrix}$	$\begin{pmatrix} W_{\mathbf{b}} & 0_{3 \times 3} \\ W_{\mathbf{s}} & 0_{3 \times 3} \\ 0_{3 \times 3} & E_{3 \times 3} \end{pmatrix}$
		$\begin{pmatrix} \lambda \\ \omega \\ \Delta \omega \end{pmatrix}$	$\begin{pmatrix} W_{\mathbf{b}} & 0_{3 \times 3} & 0_{3 \times 3} \\ W_{\mathbf{s}} & 0_{3 \times 3} & 0_{3 \times 3} \\ 0_{3 \times 3} & E_{3 \times 3} & E_{3 \times 3} \end{pmatrix}$
		$\begin{pmatrix} \lambda \\ \omega \\ \Delta \mathbf{b} \end{pmatrix}$	$\begin{pmatrix} W_{\mathbf{b}} & 0_{3 \times 3} & E_{3 \times 3} \\ W_{\mathbf{s}} & 0_{3 \times 3} & 0_{3 \times 3} \\ 0_{3 \times 3} & E_{3 \times 3} & 0_{3 \times 3} \end{pmatrix}$
Star sensor, gyro	$\begin{pmatrix} \lambda \\ \omega \end{pmatrix}$	$\begin{pmatrix} \lambda \\ \omega \end{pmatrix}$	$\begin{pmatrix} E_{3 \times 3} & 0_{3 \times 3} \\ 0_{3 \times 3} & E_{3 \times 3} \end{pmatrix}$
		$\begin{pmatrix} \lambda \\ \omega \\ \Delta \omega \end{pmatrix}$	$\begin{pmatrix} E_{3 \times 3} & 0_{3 \times 3} & 0_{3 \times 3} \\ 0_{3 \times 3} & E_{3 \times 3} & E_{3 \times 3} \end{pmatrix}$
Magnetometer, sun sensors	$\begin{pmatrix} \mathbf{b} \\ \mathbf{s} \end{pmatrix}$	$\begin{pmatrix} \lambda \\ \omega \end{pmatrix}$	$\begin{pmatrix} W_{\mathbf{b}} & 0_{3 \times 3} \\ W_{\mathbf{s}} & 0_{3 \times 3} \end{pmatrix}$
Magnetometer, gyro	$\begin{pmatrix} \mathbf{b} \\ \omega \end{pmatrix}$	$\begin{pmatrix} \lambda \\ \omega \end{pmatrix}$	$\begin{pmatrix} W_{\mathbf{b}} & 0_{3 \times 3} \\ 0_{3 \times 3} & E_{3 \times 3} \end{pmatrix}$
Star sensor	λ	$\begin{pmatrix} \lambda \\ \omega \end{pmatrix}$	$E_{3 \times 3}$

REFERENCES

- ¹ Gelb, A., *Applied Optimal Estimation*, The M.I.T. Press, Cambridge, Massachusetts, 1974.
- ² Maybeck, P., *Stochastic Models, Estimation, and Control*, N.Y.: Acad. Press. Inc, 1979.

- ³ Maybeck, P. S., "Performance Analysis of a Particularly Simple Kalman Filter," *Journal of Guidance, Control, and Dynamics*, vol. 1, Nov. 1978, pp. 391–396.
- ⁴ Tortora, P., Oshman, Y., and Santono, F., "Spacecraft Angular Rate Estimation from Magnetometer Data Only Using an Analytic Predictor," *Journal of Guidance, Control, and Dynamics*, vol. 27, May 2004, pp. 365–373.
- ⁵ Oshman, Y., and Shaviv, I., "Optimal Tuning of a Kalman Filter Using Genetic Algorithms," *AIAA Paper 2000-4558*, 2000, p. 20.
- ⁶ Powell, T. D., "Automated Tuning of an Extended Kalman Filter Using the Downhill Simplex Algorithm Introduction," *Journal of Guidance, Control and Dynamics*, vol. 25, 2002, pp. 901–908.
- ⁷ Golovan, A. A., and Parusnikov, N. A., *Navigation system matimatical foundation. Part II. Optimal estimation methods applications for navigation problems*, Moscow: Moscow University, 2008.
- ⁸ Balakrishnan, A. V., *Kalman filtering theory*, N.Y.: Optimization Software, Inc., 1987.
- ⁹ R.L. Farrenkopf, "Analytic Steady-State Accuracy Solutions for Two Common Spacecraft Attitude Estimators," *Journal of Guidance, Control, and Dynamics*, vol. 1, 1978, pp. 282–284.
- ¹⁰ Markley, F. L., "Analytic Steady-State Accuracy of a Spacecraft Attitude Estimator," *Journal of Guidance, Control and Dynamics*, vol. 23, 2000, pp. 23–25.
- ¹¹ Gai, E., Daly, K., Harrisdn, J., and Lemos, L., "Star-Sensor-Based Satellite Attitude / Attitude Rate Estimator," *Journal of Guidance, Control and Dynamics*, vol. 8, 1985, pp. 560–565.
- ¹² Xiong, K., Liang, T., and Yongjun, L., "Multiple model Kalman filter for attitude determination of precision pointing spacecraft," *Acta Astronautica*, vol. 68, Apr. 2011, pp. 843–852.
- ¹³ Springmann, J. C., Sloboda, A. J., Klesh, A. T., Bennett, M. W., and Cutler, J. W., "The attitude determination system of the RAX satellite," *Acta Astronautica*, vol. 75, Jun. 2012, pp. 120–135.
- ¹⁴ Lefferts, E. J., Markley, F. L., and Shuster, M. D., "Kalman Filtering for Spacecraft Attitude Estimation," *Journal of Guidance, Control, and Dynamics*, vol. 5, 1982, pp. 417–429.
- ¹⁵ Pittelkau, M. E., "Kalman Filtering for Spacecraft System Alignment Calibration Introduction," vol. 24, 2001, pp. 1187–1195.
- ¹⁶ Searcy, J. D., and Pernicka, H. J., "Magnetometer-Only Attitude Determination Using Novel Two-Step Kalman Filter Approach," *Journal of Guidance, Control, and Dynamics*, vol. 35, Nov. 2012, pp. 1693–1701.
- ¹⁷ Psiaki, M. L., Martel, F., and Pal, P. K., "Three-axis attitude determination via Kalman filtering of magnetometer data," *Journal of Guidance, Control, and Dynamics*, vol. 13, May 1990, pp. 506–514.
- ¹⁸ Bar-Itzhack, Y., Idanf, M., Introduction, I., and Missions, A. E., "Recursive Attitude Determination from Vector Observations : Euler Angle Estimation," *Journal of Guidance, Control, and Dynamics*, vol. 10, 1987, pp. 152–157.
- ¹⁹ Bar-Itzhack, I. Y., and Oshman, Y., "Attitude Determination from Vector Observations: Quaternion Estimation," *IEEE Transaction on Aerospace and Electronic Systems*, vol. 21, 1985, pp. 128–135.
- ²⁰ Kalman, R. E., "A New Approach to Linear Filtering and Prediction Problems," *Transactions of ASME, Series D, Journal of Basic Engineering*, vol. 82, 1960, pp. 35–45.
- ²¹ A.A. Golovan, N.A. Parusnikov, *Navigation System Mathematical Foundation. Part II. Optimal Estimation Methods Applications for Navigation Problems*, Moscow University Publications, Moscow, 2008, 128p.